Precision Scintillation Distance Measurements

Siqi Liu[1,3]★, Ue-Li Pen[1,2]†, J-P Macquart[4]‡, Walter Brisken[5]§, Adam Deller[6]¶

[1] Canadian Institute for Theoretical Astrophysics, University of Toronto, M5S 3H8 Ontario, Canada
[2] Canadian Institute for Advanced Research, Program in Cosmology and Gravitation
[3] Department of Astronomy and Astrophysics, University of Toronto, M5S 3H4, Ontario, Canada
[4] ICRAR-Curtin University of Technology, Department of Imaging and Applied Physics, GPO Box U1978, Perth, Western Australia 6102, USA
[5] National Radio Astronomy Observatory, P.O. Box O, Socorro, NM 87801, USA
[6] ASTRON, the Netherlands Institute for Radio Astronomy, Postbus 2, 7990 AA, Dwingeloo, The Netherlands

10 April 2015

ABSTRACT

We show how interstellar scintillations, combined with VLBI measurements, can be used to measure pulsar distances. Two lensing screens are needed. We apply the technique to archival data on PSR B0834+06. Rough distance estimates, consistent with direct parallax measurements, are obtained. If observations over a six month period had been made at that epoch, we anticipate a 1% distance determination.

With longer ground-based baselines and wider frequency coverage, we speculate that distance determination perhaps as accurate as 0.1% could be possible. This would enable coherent pulsar gravitational wave timing and imaging.

Key words: Pulsar

1 INTRODUCTION

Pulsars have long provided a rich source of astrophysical information due to their compact emission and predictable timing. One of the weakest measurements for most pulsars is their direct geometric distance. For some pulsars, timing parallax or VLBI parallax has resulted in direct distance determinations. For most pulsars, the distance is a major uncertainty for precision timing interpretations, including mass, moment of inertia, and gravitational wave direction(Boyle & Pen 2012).

Direct VLBI observation of PSR B0834+06 shows multiple images lensed by the interstellar plasma. Combining the angular positions and scintillation delays, the authors published the derived effective distance (Brisken et al. 2010) of approximately 1168 ± 23 pc for apexes whose time delays range from 0.1 ms to 0.4 ms, and 1121 ± 59 pc for 1 ms apexes. This represents a precise measurement compared to all other attempts to derive distances to this pulsar. This effective distance is a combination of pulsar-screen and earth-screen distances, and does not allow a separate determination of the individual distances.

A second lensing screen breaks the degeneracy.

★ E-mail: sqliu@cita.utoronto.ca
† E-mail: pen@cita.utoronto.ca
‡ E-mail:J.Macquart@curtin.edu.au
§ Email:wbrisken@aoc.nrao.edu
¶ E-mail:deller@astron.nl

2 LENSING

To break the degeneracy of the result and know the accurate distance of the pulsar, we dealt with the archival data of B0834. We selected the apexes from four band, centering 314.5 MHz, 322.5 MHz, 328.5MHz and 334.5MHz, all with a bandwidth of 8 MHz. Separating them into two piles, one with time delay ranges from 0.1 ms to 0.4 ms, the other with time delay of 1 ms. Plotting those apex points on a f_D-τ plane, we match the points which are adjacent to each other. Thus we seleted 9 apex positions from the 1ms cluster, and 5 apex positions from the 0.4 ms cluster. How distance is related to the time delay and how velocity is related to the differential frequency is defined by the following equations:

$$\tau = \frac{D_e \theta^2}{2c},$$
$$f_D = f \cdot \frac{\delta\tau}{dt},$$

where D_e is the effective distance, equivalent to the lens placing at the middle point of the pulsar: $D_e = D_p D_s/(D_p - D_s)$.

From τ, RA and dec, we obtained the result that the positions of the pulsar: for 0.4 ms pile, $D_e = 1017 \pm 2.8$ pc; and for 1 ms pile, $D_e = 1121 \pm 64$ pc. Thus, the degeneracy is broken. Furthermore, if we know the distance of the pulsar is 640 pc by parallax, the screen where 0.4 ms scintellation points are deflected, D_s is equivalent to 392.82 pc. Then

with the angle of the axis 25.2 degree west of north, we get the calculated RA and dec.

Similarly, for 1 ms pile, the D_s is equivalent to 422.5 pc and is calulated the RA and dec.

Then we fit a line to this five calculated points. Lying on the fitted line, point 5 is obtained with equal $\theta_\parallel$ as the farthest point in the 0.4 ms pile. Knowing the differential frequency f_D of this point, we know the relative velocity of this point to the pulsar, called vA5, which is in the direction away from the screen image opposite to the position of the pulsar. Similarly, we obtained the $v_\parallel$ from the 0.4 ms data. Thus, the total velocity of the pulsar is determined. Knowing τ , we can get the angle of the screen image away from the pulsar. Knowing the line and the differential frequency, we can get the ra and dec of the pulsar.

That is one lens model fitting.

But according to Fermat's law, the distributions of the pile of 1ms points are not reasonable. If they are being reflected by one interstellar medium lens, they should be distributed along a line like the 0.4 ms pile, just lie in the direction of the pulsar and point J in 2.

We calculated the $\theta_\parallel$ of the respective RA and dec positions to the 0.4ms axis. And we got five matched positions, which is marked on 2.

One alternative explanation of this is: the 1 ms pile of points are the result of double lens. First deflected and then reflected. Solved positions are plotted in 2. By Fermat's law, the velocity parallel to the lens plane should be equal.

We made a plot of the reflected velocity in the direction that is transverse to the first lens plane in 3. From our calculation, it takes 22 days for the injectioned image of the puslar on the far screen to move to the first apex position, and it takes 44 days of the injected image of the pulsar on the far screen from J to move to the fifth apex position.

3   B0834+06

Our analysis is based on the reduced apex catalog from Brisken et al. (2010). Each identified apex includes a delay, delay rate, RA and Dec, one for each of 4 frequency bands. We mapped a total of 9 apexes from the 0.4ms cluster, and 5 from the 1ms cluster, across the 4 frequency bands. This results in an estimate for the mean value, and standard deviation. These are listed in Table 3. The time is calculated with $2\tau f/f_D$, which is equivalent to pulsar moving at 640pc plane from the original position to the lensed image angle with the velocity calculated. A least squares effective distance results in $D_e^M = 1017 \pm 2.8$ for the main 0.4ms cluster and $D_e^S = 1243 \pm 64.1$ for the secondary 1ms cluster. This seems to indicate that the secondary screen is closer to the pulsar. The error bars are large enough to allow them to be at the same distance, or perhaps a reverse distance ordering. In this paper, we present two analyses for comparison: equidistant, and at the best fit distances. In the first case, no direct distance measurement is possible, but it nevertheless illustrates a robust interpretation of the data.

4   LENS SOLUTION

In order to interpret the data, we adopt the lensing model of Pen & Levin (2014). In the absence of a lens model, the fringe rate, delay and angular position cannot be uniquely related. In this model, the lensing is due to projected fold caustics of a thin sheet closely aligned to the line of sight.

5   DISCUSSION

The lens solution appears consistent with the premise of the inclined sheet lensing model(Pen & Levin 2014). The secondary lens only images a subset of the primary lens images. This could happen if the secondary lens screen is just under the critical inclination angle, such that only $3-\sigma$ waves lead to a fold caustic. If the primary lens were at a critical angle, the chance of encountering a somewhat less inclined system is of order unity.

More surprising is the absence of a single deflection image of the pulsar, which is expected at position J. This could happen if the maximum deflection angle is just below critical, such that only rays on the appropriately aligned double deflection can form images. This scenario predicts that at frequencies just below 300 MHz, or a few weeks earlier in time, the pulsar should be seen at position J.

6   POSSIBLE IMPROVEMENTS

We discuss several strategies which can improve on the solution accuracy. The single biggest improvement would be to monitor over a week, when the pulsar crosses each individual lens, including both lensing systems.

Angular resolution can be improved using longer baselines, for example adding a GMRT-GBT baseline doubles the resolution. Observing at multiple frequencies over a longer period allows for a more precise measurement: when the pulsar is between two lenses, the deflection angle is small, and one expects to see the lensing at higher frequency, where the resolution is higher, and distances between lenses positions can be measured to much higher accuracy.

Holographic techniques(Walker et al. 2008; Pen et al. 2014) may be able to measure delays, fringe rates, and VLBI positions sbstantially more accurately. Combining these techniques, the interstellar lensing could conceivably achieve distance measurements an order of magnitude better than the current published effective distance errors. This could bring most pulsar timing array targets into the coherent timing regime, enabling arc minute localization of gravitational wave sources, lifting any potential source confusion.

Ultimately, the precision of the lensing results would be limited by the fidelity of the lensing model. In the inclined sheet model, the images move along fold caustics. The straightness of these caustics depends on the inclination angle, which in turn depends on the amplitude of the surface waves.

7   CONCLUSIONS

We have presented a new technique of two plane interstellar plasma lensing to determine distances to pulsars. We have

f_D(mHz)	σ_{f_D}(mHz)	τ(ms)	σ_τ(ms)	RA(mas)	σ_{RA}(mas)	dec(mas)	σ_{dec}(mas)	time(day)
-12.94	0.19	0.0845	0.0005	2.87	0.11	-8.2	0.09	49.9
-16.8	0.28	0.14125	0.00085	3.86	0.07	-10.6	0.05	64.5
-18.92	0.23	0.188	0.002	5.06	0.2	-10.6	0.13	74.4
-20.4	0.49	0.222	0.003	5.55	0.3	-11.7	0.21	80.8
-21.17	0.61	0.236	0.002	5.12	0.43	-12.6	0.31	83.4
-22.32	0.47	0.2633	0.0003	6.16	0.14	-14.2	0.1	88.0
-24.63	0.4	0.3265	0.0025	6.49	0.29	-14.1	0.2	98.0
-24.94	0.44	0.33775	0.00025	8.29	0.42	-14.4	0.32	99.7
-26.09	0.36	0.37425	0.00063	8.53	0.52	-15.7	0.42	105
-35.06	0.52	0.95	0.002	-15.23	0.69	-21.06	0.7	202
-38.31	0.64	0.976	0.0009	-15.02	0.485	-20.74	0.38	190
-40.17	0.55	1.005	0.0079	-14.14	0.662	-22.27	0.62	187
-41.27	0.54	1.037	0.003	-11.28	0.93	-19.18	1.1	188
-43.08	0.44	1.066	0.005	-8.41	1.7	-24.14	1.4	185

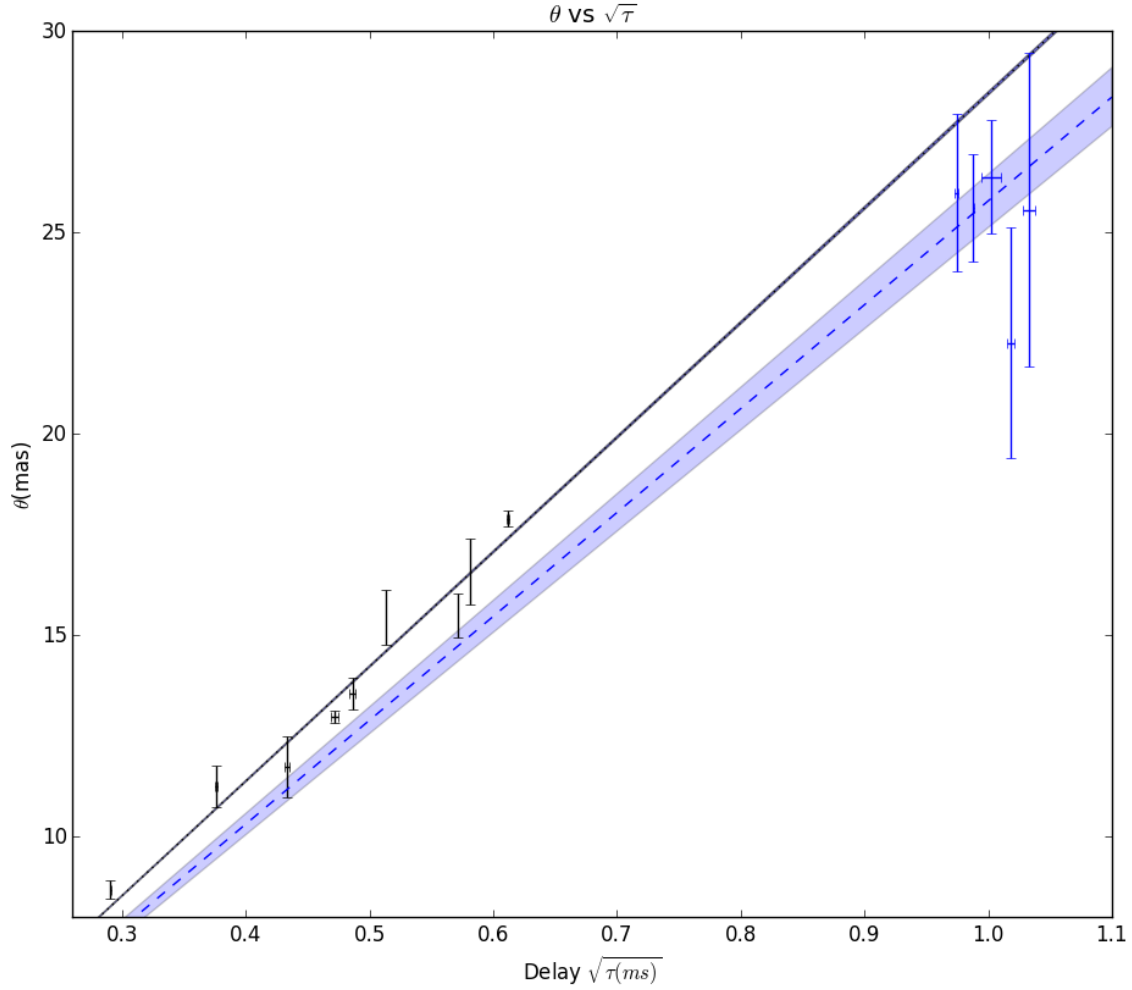**Table 1.** 0.4ms and 1ms observation positions.

Figure 1. θ vs $\sqrt{\tau}$. The black line is the fitted line of the 0.4ms positions, where $k = 28.51$. The blue lines are the fitted lines of the 1ms position, where $k = 25.784$ with an error region of $\sigma_k = 0.66$.
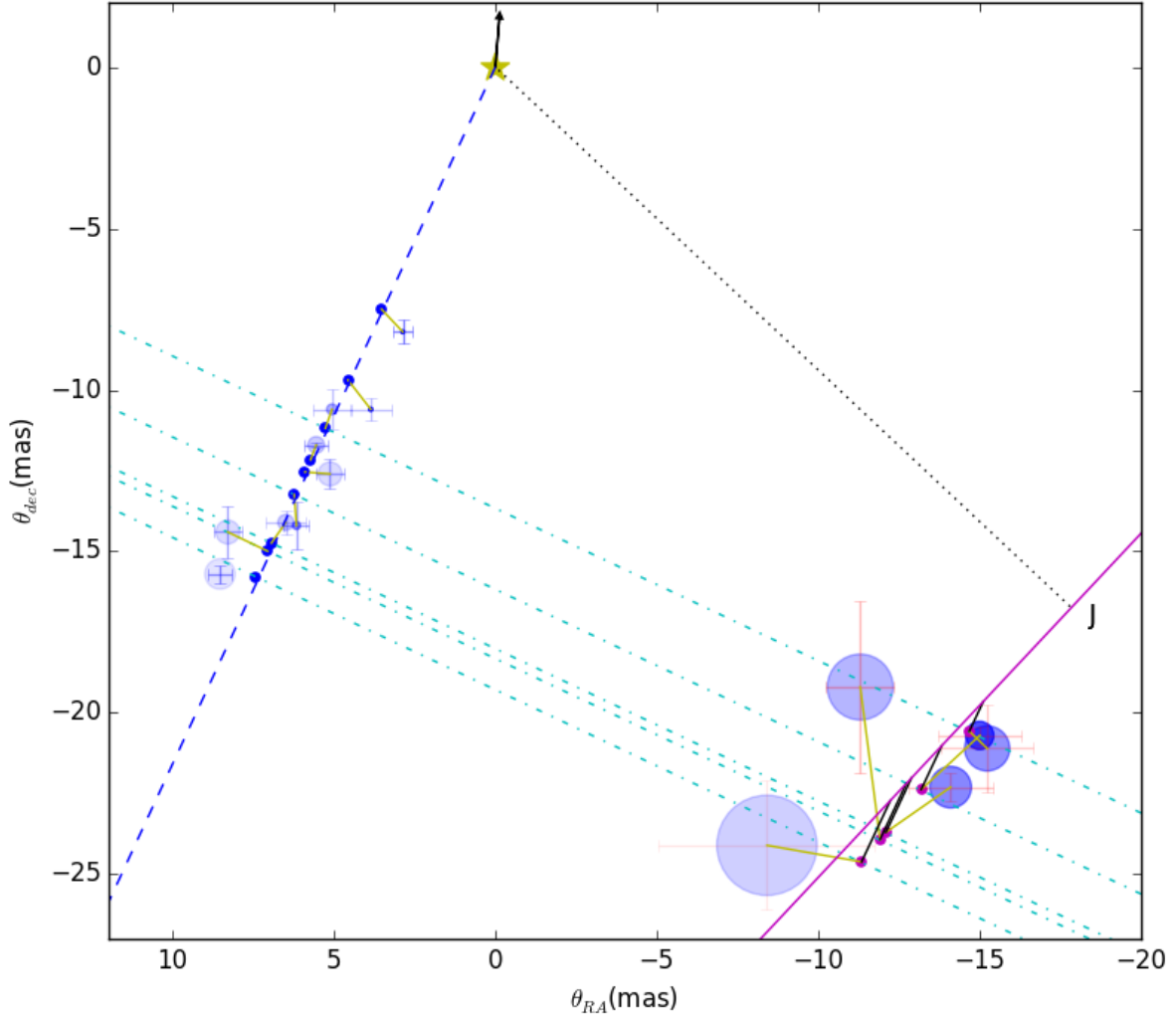
Figure 2. Fitted position of 1ms and 0.4ms data of double lens model and observation data.In both apexes regions, the position of the screen locate at 392.82pc and 425pc. Blue points on the left side are the points that fitted from the f_D and τ of from the 0.4ms observation. Blue line is the fitted line of 0.4ms apex positions, with a 25.2 degree west of the north. The points lie on the left side with errorbars, are the observation points together with their sample errors; while the transparent circles are plotted with population errors, where smaller transparent data are darker. Short solid lines between them are the matched positions of the apexes in $1ms$ region and $0.4ms$ region, which share the same $\theta_\parallel$. The points on the right side are the points that fitted from the f_D and τ of the 1ms observation with an avearage of four bandwidths. Solid line is the fitted line of these positions. Those points with errorbars nearby are the observation points together with their sample errors, while the transparent circles are plotted with population errors. The dotted line on the top right side is vertical to the solid line. Short solid lines connect the observation points and the fitted positions. Middle lines connect the 0.4ms and 1ms fitted positions with the same $\theta_\parallel$. The velocity of the pulsar is 191.4km/s, with a degree 5.56 degree west of north, is also marked out at the top of the figure.
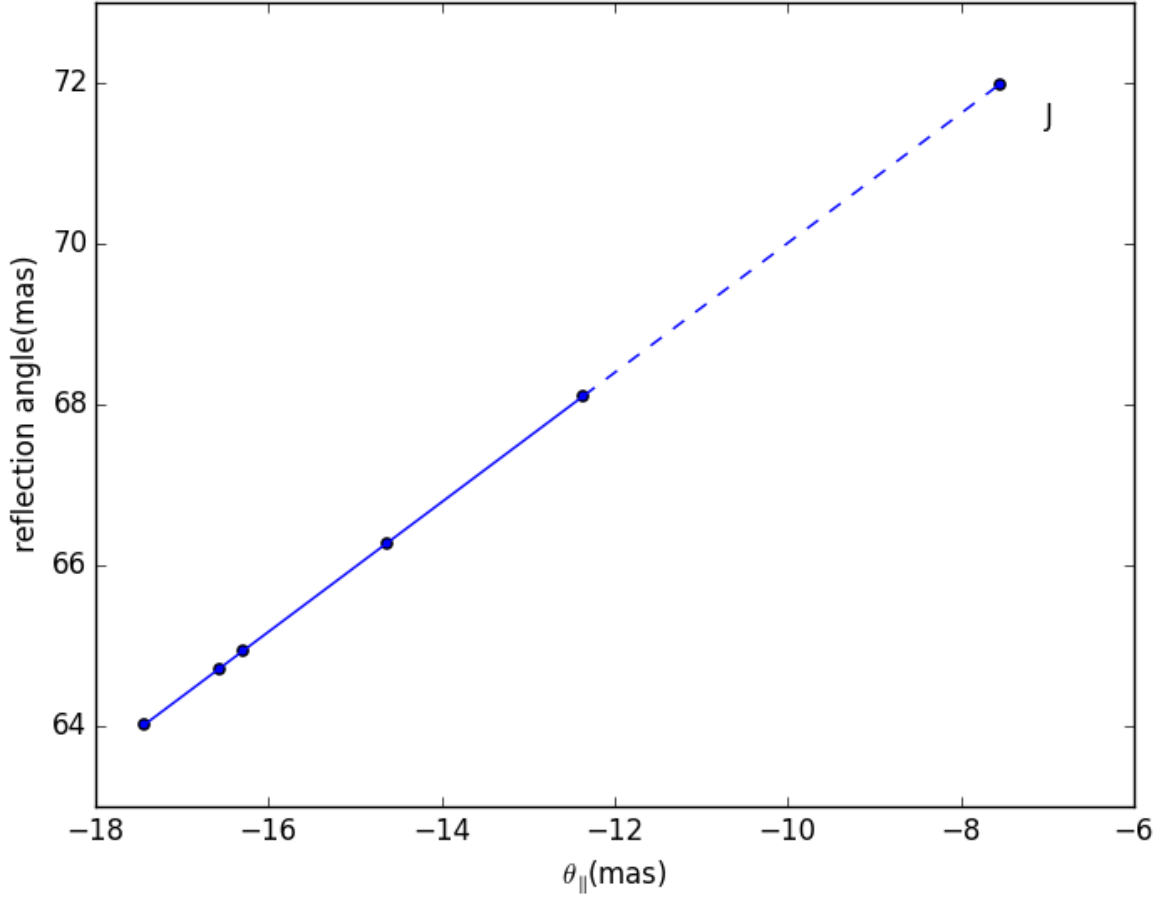
Figure 3. Injection velocity minus reflected velocity over the speed of light. J specifically marked in the paper.

tested this approach on archival data, showing that in principle solutions can be obtained. We conclude that multi-epoch observations over weeks, at a range of frequencies, might result in much more accurate distance determinations.

8 ACKNOWLEDGEMENTS

REFERENCES

Boyle L., Pen U.-L., 2012, Phys. Rev. D, 86, 124028
Brisken W. F., Macquart J.-P., Gao J. J., Rickett B. J., Coles W. A., Deller A. T., Tingay S. J., West C. J., 2010, ApJ, 708, 232
Pen U.-L., Levin Y., 2014, MNRAS, 442, 3338
Pen U.-L., Macquart J.-P., Deller A. T., Brisken W., 2014, MNRAS, 440, L36
Walker M. A., Koopmans L. V. E., Stinebring D. R., van Straten W., 2008, MNRAS, 388, 1214